PAPER

A Maximum Likelihood Decision Based Nonlinear Distortion Compensator for Multi-Carrier Modulated Signals

Minoru OKADA[†], **Hideki NISHIJIMA**[†*], *and* **Shozo KOMAKI**[†], *Members*

SUMMARY This paper proposes a new nonlinear distortion compensation scheme for orthogonal multi-carrier modulation systems. Multi-carrier modulation is an effective technique for high speed digital transmission over time-dispersive channels, however, it is very sensitive to nonlinear distortion. The proposed scheme compensates for the performance degradation due to nonlinear distortion using the maximum likelihood (ML) detection criterion. While the ideal ML receiver requires a huge computational cost and is not feasible, the proposed decision algorithm can effectively reduce the computational cost. Instead of evaluating the likelihood function for all the possible sequences, the proposed scheme examines the sequences which differ by only one bit from the sequence decoded by the conventional receiver. Computer simulation results show that the proposed scheme can effectively compensate for the nonlinear distortion.

key words: *multi-carrier modulation, nonlinear distortion, MLSE*

1. Introduction

Orthogonal multi-carrier modulation, also referred to as "orthogonal frequency division multiplexing (OFDM)," is an effective technique for high speed digital transmission over time-dispersive channels, and has been suggested for a variety of applications such as digital transmission over telephone line or "high bit rate digital subscriber line (HDSL)" transmission [1], terrestrial and satellite digital broadcasting system [2], [3] and wireless local area networks [4]. In multi-carrier modulation systems, although each sub-carrier operates at low data rate against time-dispersion, the total high data rate transmission can be achieved by using multiple sub-carriers.

As mentioned above, a lot of attention has been paid to the multi-carrier modulation in a variety of applications, however, it has a main drawback, that is, a sensitivity to nonlinear distortion due to high power amplifier (HPA) [3], [5]–[7]. Since the multi-carrier modulated signal is the sum of a large number of (several hundreds) modulated sub-carriers, its amplitude widely varies even if the amplitude of each modulated sub-carrier has a constant envelope. Because of this amplitude variation, the multi-carrier signal is severely distorted by the nonlinearity of HPA which leads out-of-band emission and the bit error rate (BER) performance degradation.

Out-of-band emission is a serious problem in radio communication systems especially in a band limited environment, because it makes adjacent channel interference. For multi-carrier modulated signal, it has been suggested in [8] that this can be solved by using techniques such as a low peak power transmission technique. On the other hand, in HDSL system, optical fiber radio extension link [9], and some satellite communication systems where there is no adjacent channel or bandwidth is not severely limited, out-of-band emission is not a serious problem. This implies that we do not have to always pay attention to the out-of-band emission in conjunction with nonlinear amplification.

On the other hand, to reduce the performance degradation due to nonlinear amplification, the operating point in HPA must be largely backed off from the saturation point. However, backing off the operating point also reduces the output power and the power efficiency of the HPA. In a portable transmitter or a satellite transponder where the power consumption is strictly limited, it is not acceptable. Therefore, in order to improve the BER performance in nonlinear environment, some techniques have been proposed, for instance, a postdistortion receiver for mobile communications has been discussed in [10], and postdistortion-type nonlinear distortion compensator for sub-carrier modulation (SCM) optical transmission system in [11]. However, there has been no study on nonlinear distortion compensator for orthogonal multi-carrier modulation system. Fortunately, since all the sub-carriers in multi-carrier modulation are modulated synchronously, more sophisticated detection techniques such as maximum likelihood sequence estimation could be easily applied to the receiver.

In this paper, we propose a new nonlinear distortion compensation scheme for orthogonal multi-carrier modulation systems. The proposed compensator is based on a maximum likelihood (ML) detection at the receiver. The receiver with the proposed nonlinear distortion compensator generates replicas of the possible transmitted signals with nonlinear distortion and selects

Manuscript received February 13, 1997.
Manuscript revised August 26, 1997.

[†]The authors are with the Faculty of Engineering, Osaka University, Suita-shi, 565–0871 Japan.
[*]Presently, NTT Kansai Mobile Communications Network, Inc.

a replica which is the closest to the received signal. Although the ML detection is optimum, it is impossible to implement, because the computational cost increases rapidly with the number of sub-carriers if all the possible replicas are evaluated. To reduce the computational cost, we propose a sub-optimum detection procedure. Instead of evaluating all the possible replicas, the proposed procedure only evaluates replicas which differ only one bit from the binary sequence which is demodulated by the conventional multi-carrier receiver. The computational cost of the proposed scheme is relatively small as compared with the complete ML detection procedure. Moreover, by repeating this procedure, the proposed scheme can further improve the BER performance.

This paper is organized as follows: Section 2 describes the orthogonal multi-carrier modulation system model, Sect. 3 shows a nonlinear distortion compensator based on the maximum likelihood criterion. Section 4 theoretically analyzes the bit error rate performance of the maximum likelihood receiver. Section 5 proposes a new sub-optimum nonlinear distortion compensator, which can reduce the computational cost of the maximum likelihood compensator. Finally, Sect. 6 shows computer simulation and numerical results on the BER performance.

2. System Description

Figure 1 illustrates the block diagram of the orthogonal multi-carrier modulation system discussed in this paper.

Let

$$B = [b_0, b_1, \ldots, b_{KN-1}] = [\mathbf{b}_0, \mathbf{b}_1, \ldots, \mathbf{b}_N], \tag{1}$$

be a binary information sequence composed of KN information bits where

$$\mathbf{b}_k = [b_{kN}, b_{kN+1}, \ldots, b_{kN+K-1}], \tag{2}$$

is a sub-sequence of B. The sequence B is applied to the 2^K-ary QAM (quadrature amplitude modulation) modulator, and here the k-th output of the modulator is given by

$$c_k = Q(\mathbf{b}_k), \tag{3}$$

where $Q(\mathbf{b})$ is the mapping of the QAM modulator. The output of the QAM modulator c_k is then applied to the serial to parallel converter (S/P), where N QAM symbols are parallelly processed. Here, the output of S/P is given by

$$C = [c_0, c_1, \ldots, c_{N-1}]. \tag{4}$$

The output C is then applied to the inverse discrete Fourier transform (IDFT) processor, where the N modulated sub-carriers with different sub-carrier frequencies are summed up by the IDFT. Defining t_s as the observation period (symbol period) of the IDFT, all the sub-carriers are spaced by $1/t_s$ in the frequency band, and the frequency of the k-th sub-carrier is given by

$$f_k = \frac{k}{t_s} + f_l, \tag{5}$$

where f_l is the lowest sub-carrier frequency. The multi-carrier modulated signal without nonlinear distortion in the transmitter is given by

$$s(t) = \sum_{k=0}^{N-1} c_k \exp(j2\pi f_k t). \tag{6}$$

Through the nonlinear amplifier, $s(t)$ experiences a nonlinear distortion, and the output signal from the transmitter is given by

$$s_0(t) = g_c(s(t)), \tag{7}$$

where

$$g_c(x) = g(|x|)e^{j[\angle x + f(|x|)]}, \tag{8}$$

is the input/output characteristic function, $|x|$ and $\angle x$ are the amplitude and the phase of x, respectively, and $g(x)$ and $f(x)$ are the amplitude and phase characteristics of the nonlinear HPA, respectively.

Now, we focus our attention to the following solid state power amplifier (SSPA) as the nonlinear HPA in the transmitter. The amplitude and phase characteristics of the SSPA are given by [6]

$$g(x) = \frac{x}{(1 + x^{2p})^{1/2p}}, \tag{9}$$

and

$$f(x) = 0, \tag{10}$$

where p is the smoothing factor of the transition from the linear region to the limiting region. The operating point of the amplifier is expressed as the back-off, and the input back-off and output back-off are defined as:

$$IBO = 10\log_{10}\frac{P_{i,sat}}{P_i}, \tag{11}$$

and

$$OBO = 10\log_{10}\frac{P_{o,sat}}{P_o}, \tag{12}$$

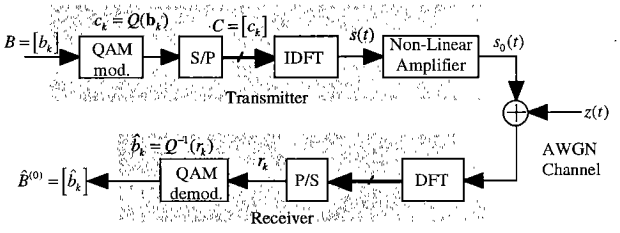

Fig. 1 Block diagrams of the orthogonal multi-carrier modulation transmitter and receiver.

where P_i and P_o are the average powers at the input and output of the HPA, respectively. $P_{o,sat}$ is the saturation output power and $P_{i,sat}$ is the input power corresponding to the saturation point.

The received signal is given by

$$r(t) = s_0(t) + z(t), \tag{13}$$

where $z(t)$ is a complex Gaussian noise component added through the channel. The received signal is then applied to the discrete Fourier transform (DFT) processor. The k-th sub-carrier component is given by

$$\begin{aligned} r_k &= \frac{1}{t_s}\int_0^{t_s} r(t)\exp(-j2\pi kt)dt \\ &= c_k + z_k + u_k, \end{aligned} \tag{14}$$

where

$$z_k = \frac{1}{t_s}\int_0^{t_s} z(t)\exp(-j2\pi kt)dt, \tag{15}$$

is the complex Gaussian noise component corresponding to the k-th sub-carrier, and u_k is the crosstalk, namely, the adjacent sub-channel interference component due to the nonlinear distortion.

At the final stage in the receiver, the symbol-by-symbol detector estimates the transmitted binary sequence. The output of the detector is given by

$$\hat{\mathbf{b}}_k(=[\hat{b}_{kN}, \hat{b}_{kN+1}, \ldots, \hat{b}_{(k+1)N-1}]) = Q^{-1}(r_k), \tag{16}$$

where $Q^{-1}(\cdot)$ is a decision function corresponding to $Q(\cdot)$. The output binary sequence is finally given by

$$\hat{B}^{(0)} = [\hat{\mathbf{b}}_0, \hat{\mathbf{b}}_1, \ldots, \hat{\mathbf{b}}_N], \tag{17}$$

where we call this receiver based on the decision rule given by (16) "a conventional receiver."

In the symbol by symbol detector expressed above, the term u_k performs as an additive noise component, and degrades the BER performance. However, since u_k is a function of $C = [c_0, \ldots, c_{N-1}]$, the degradation can be effectively compensated for by exploiting the information of u_k.

3. Maximum Likelihood Nonlinear Distortion Compensator

This section describes the maximum likelihood nonlinear distortion compensator. Since the effect of u_k in (14) is taken into account, the ML compensator can compensate for the BER degradation due to nonlinear distortion.

Let $\hat{s}_0(t; B)$ be a replica of the transmitted signal when the sequence B is transmitted and let

$$\hat{r}_k(B) = \frac{1}{t_s}\int_0^{t_s} \hat{s}_0(t; B)\exp(-j2\pi kt)\,dt, \tag{18}$$

be the expected received signal corresponding to $\hat{s}_0(t; B)$, where $\hat{r}_k(B)$ corresponds to the term $c_k + u_k$ in (14) when B is transmitted. The detector first calculates the likelihood function on all the possible sequences. Since the channel is supposed to be an AWGN channel, the likelihood function can be expressed by the Euclidean distance:

$$d(B) = \sum_{k=0}^{N-1} |r_k - \hat{r}_k(B)|^2. \tag{19}$$

The ML detector determines the sequence $\hat{B}$ which minimizes the Euclidean distance, i.e., $\hat{B}$ satisfies

$$d(\hat{B}) = \min_B d(B). \tag{20}$$

4. Theoretical Analysis

In this section, we theoretically derive the bit error rate performance of the ML receiver. Since $s(t)$ in (6) is the sum of many sub-carriers, $s(t)$ can be approximated as a Gaussian noise whose power spectrum density is

$$W(f) = \begin{cases} \dfrac{P_i}{B}; & |f| \leqq B/2 \\ 0; & |f| > B/2 \end{cases}, \tag{21}$$

where $B = N/t_s$ is the bandwidth of the signal.

The desired signal component of the output of the nonlinear device is given by [5]

$$W_1(f) = A_1 W(f), \tag{22}$$

where

$$A_1 = \left|\frac{1}{2\sigma_i}\int_0^{\infty} \rho^2 e^{-\rho^2/2} g(\sigma_i\rho) e^{jf(\sigma_i\rho)} d\rho\right|^2, \tag{23}$$

and $\sigma_i = \sqrt{P_i}$. The third order inter-modulation component (IM3) corresponding to u_k in (14) is given by [5]

$$W_3(f) = A_3(W \otimes W \otimes W)(f), \tag{24}$$

where $\otimes$ denotes the convolution, and

$$\begin{aligned} A_3 &= \frac{1}{8}\left|\frac{1}{\sigma_i^3}\int_0^{\infty} \rho^2\left(\frac{\rho^2}{2} - 2\right) e^{-\rho^2/2} g(\sigma_i\rho) e^{jf(\sigma_i\rho)} d\rho\right|^2. \end{aligned} \tag{25}$$

If no nonlinear compensation is performed, the IM3 component performs as an additive noise component. Therefore, the effective signal-to-noise power ratio (SNR) is given by

$$\gamma_{\text{effect}} = \frac{W_d(f)}{N_0 + W_3(f)}, \tag{26}$$

where N_0 is the single-sided spectral density of the AWGN component.

Now, we are focusing on the ML detection. Let $W_m(f)$ be the power spectrum of the m-th sub-carrier component in Fig. 2 (c), and let $W_{-}(f)$ be the remaining component in Fig. 2 (b):

$$W(f) = W_m(f) + W_{-}(f). \tag{27}$$

Substituting (27) into (24), we can get

$$\begin{aligned} W_3(f) = A_3[&(W_- \otimes W_- \otimes W_-)(f) \\ &+ 3(W_- \otimes W_- \otimes W_m)(f) \\ &+ 3(W_- \otimes W_m \otimes W_m)(f) \\ &+ (W_m \otimes W_m \otimes W_m)(f)]. \end{aligned} \tag{28}$$

In this equation, the second term in Fig. 2 (d) contributes much to the detection of the m-th sub-carrier, so we neglect the third and fourth terms. We can get the power spectrum of the usable signal component as

$$W_{\mathrm{ML}}(f) = A_1 W_m(f) + 3A_3(W_- \otimes W_- \otimes W_m)(f). \tag{29}$$

Therefore, in this case, the effective SNR is given by

$$\gamma_{\mathrm{effect}}^{(\mathrm{ML})} = \frac{t_s \int_{-B/2}^{B/2} W_{\mathrm{ML}}(f)df}{N_0}. \tag{30}$$

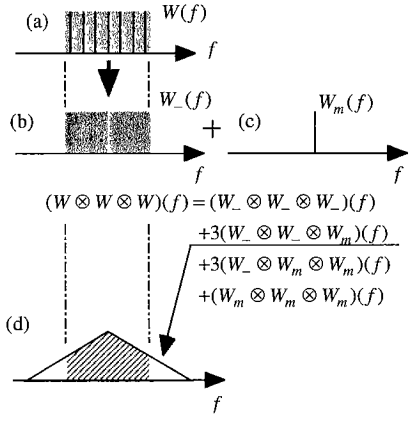

Fig. 2 Spectra of intermodulation products.

When QPSK (Quadrature Phase Shift Keying) is employed as a modulation format for each sub-carrier, the BER performance is approximated by

$$P_b \sim \frac{1}{2}\mathrm{erfc}\left(\sqrt{\frac{\gamma_{\mathrm{effect}}}{2}}\right). \tag{31}$$

5. Sub-Optimum Nonlinear Distortion Compensator

Although the ML detection is optimum on the BER performance, the computational cost increases rapidly as the number of sub-carriers and the number of modulation levels increase. If 2^K-level modulation is employed for each sub-carrier, the ML detection requires 2^{KN} evaluations of (19). This means that the ML detection is not feasible when KN is large.

To reduce the computational cost, we propose a new sub-optimum compensator. Instead of evaluating (19) for all the possible sequences, the proposed procedure evaluates only binary sequences which differ by only one bit from the sequence obtained by the conventional receiver.

The block diagram and the detection algorithm of the proposed nonlinear distortion compensator are summarized in Figs. 3 and 4, respectively. In Fig. 3, the received signal is first decoded with the conventional receiver illustrated in Sect. 2. The decoded sequence $\hat{B}^{(0)}$ is applied to the sequence generator generating KN sequences which differ by only one bit from $\hat{B}^{(0)}$.

Let $B_m^{(l+1)}$ be the binary sequence of KN bits in which only the m-th bit of $B_m^{(l+1)}$ differs from $\hat{B}^{(l)}$. The generated sequences $B_m^{(1)}$ and the original one $\hat{B}^{(0)}$ are then applied to the transmitter model, which has the same input/output characteristic of the transmitter shown in Sect. 2. The output signals of the transmitter model are then applied to the DFT(2) to generate the expected received signals corresponding to $B_m^{(1)}$ and $\hat{B}^{(0)}$. The compensator calculates the Euclidean distance between r_ks and $r_k(B_m^{(1)})$s or $r_k(\hat{B}^{(0)})$ and chooses the sequence $\hat{B}^{(1)}$ which has the minimum Euclidean distance in the distances corresponding to $B_m^{(1)}$s and $\hat{B}^{(0)}$. Although the chosen sequence is not the result of ML compensator, we have a chance to get the better sequence whose Euclidean distance is shorter than

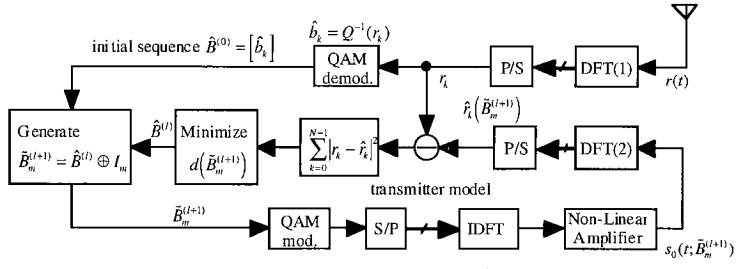

Fig. 3 Block diagram of the proposed nonlinear distortion compensator.

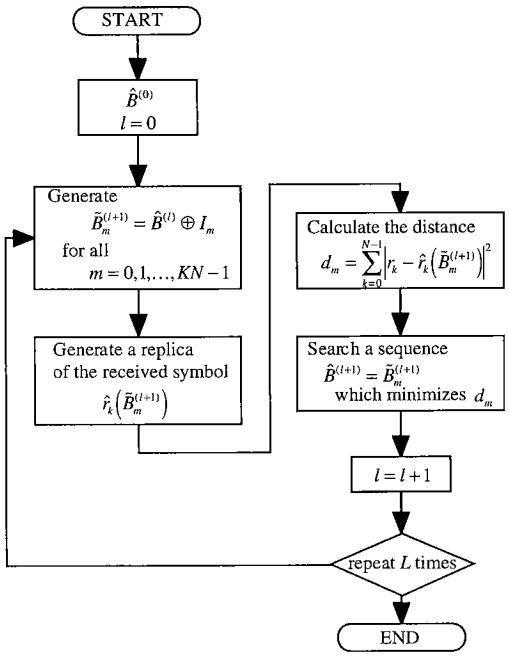

Fig. 4 Flow chart diagram of the nonlinear distortion compensation procedure.

that of the original one. Applying the chosen sequence $\hat{B}^{(1)}$ to the sequence generator to generate $B_m^{(2)}$ and repeating the procedure mentioned above, we can improve the BER performance. Furthermore, as shown in Fig. 4, sequences $B_m^{(l+1)}$ are generated from the l-th sequence $\hat{B}^{(l)}$ at $(l+1)$-th compensation step, and the compensator calculates the Euclidean distance between r_ks and $r_k(B_m^{(l+1)})$s or $r_k(\hat{B}^{(l)})$ and chooses the next sequence $\hat{B}^{(l)}$ which minimizes the Euclidean distance. Repeating this procedure, we can further improve the BER performance.

Although the proposed nonlinear distortion compensator is no longer optimum, the proposed scheme only requires $KN+1$ evaluations of (19), and is feasible even if the number of sub-carriers becomes several hundreds. Figure 5 shows the computational cost against the number of bits, NK. The computational cost is evaluated by the required number of DFT calculations in each symbol. The computational cost required for the ML receiver exponentially increases with the increase in NK, while the cost required for the proposed receiver is linearly proportional to NK and much less than that of the ML receiver in a higher NK region. This implies that the proposed scheme can drastically reduce the computational cost required for the compensation of nonlinear distortion.

6. Numerical Results

In this section, we show numerical and computer simulation results of the proposed nonlinear distortion

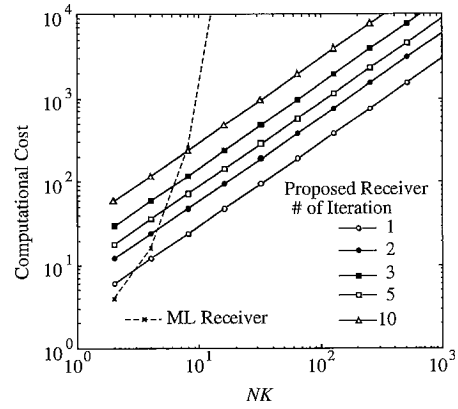

Fig. 5 Computational cost as compared with the conventional DFT based receiver without nonlinear distortion compensation.

Table 1 System parameters.

the number of subcarriers	$N = 32$
Modulation format	QPSK ($K = 2$) 16 QAM ($K = 4$)
SSPA parameter	$p = 3$

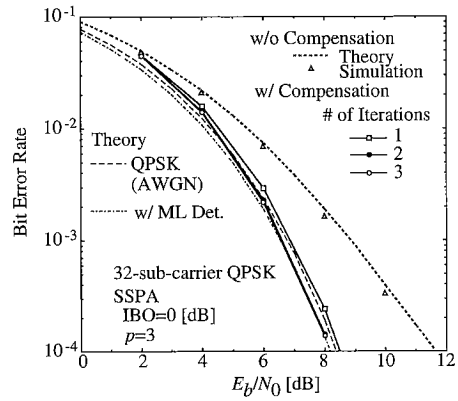

Fig. 6 Bit error rate performance of the proposed nonlinear distortion compensator for SSPA.

compensator. Table 1 shows the system parameters to demonstrate the performance. The HPAs at the transmitter and receiver have the same input/output characteristic and the same back-off level. We evaluate the BER for 5000 simulation runs in an AWGN channel.

Figure 6 is the BER performance of the 32-sub-carrier QPSK in the AWGN channel against E_b/N_0 at the input back-off level of 0 dB. The two dashed lines mean the theoretical BER without compensation in nonlinear environment, and that without compensation in linear environment, respectively, and the dash-dotted line means the theoretical BER with compensation in nonlinear environment. The proposed compensator can compensate for the BER degradation due to the nonlinear distortion caused by the SSPA, and reach to the theoretical BER for the ML receiver.

In order to investigate the required number of it-

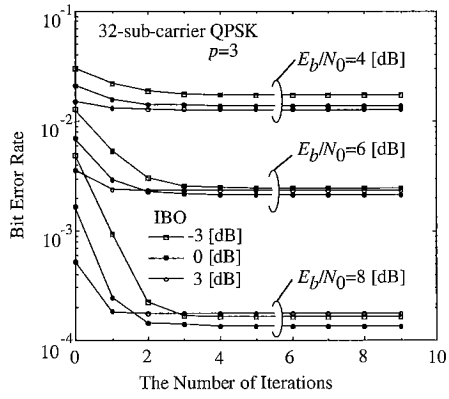

Fig. 7 Bit error rate performance against the number of iterations.

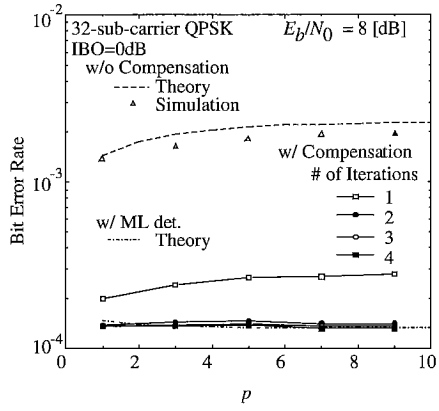

Fig. 9 Bit error rate performance against the parameter p.

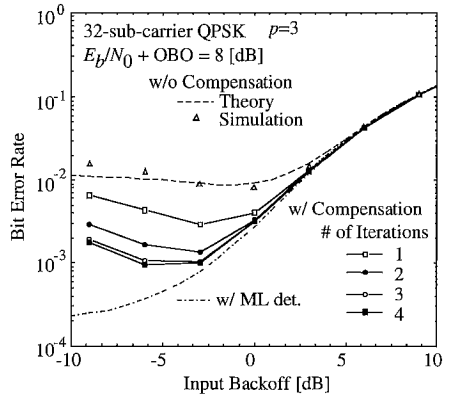

Fig. 8 Bit error rate performance against the input back-off level.

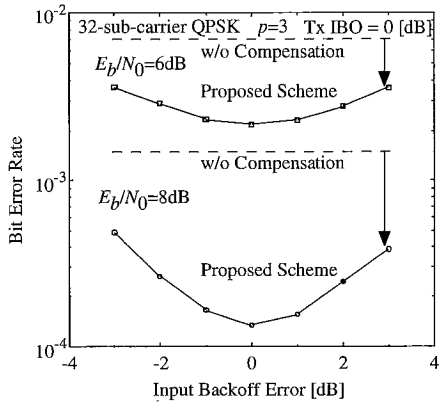

Fig. 10 Effect of the input back-off error between transmitter and receiver.

erations to compensate for the nonlinear distortion, we then show the BER performance against the number of iterations in Fig. 7. When the input back-off level is 3 dB, only one iteration is sufficient to obtain a good BER, and at most 3 iterations are required even if the input back-off level is -3 dB.

Figure 8 shows the BER performance against the input back-off level of the SSPA at $E_b/N_0 + OBO = 8$ dB. $E_b/N_0 + OBO$ in dB means the maximum E_b/N_0 when the HPA operates at the saturation point. The optimum input back-off level is 0 dB without compensation at $E_b/N_0 + OBO = 8$ dB. On the other hand, when the proposed compensator is applied, the optimum input back-off level reaches -6 dB. Therefore, the SSPA can operate at the point closer to the saturation point, in other words, the power efficiency of the SSPA can be improved by the proposed compensator. Furthermore, the bit error rate performance of the proposed compensator agrees well with the theoretical result on the ML receiver at $IBO > -3$ dB.

Figure 9 shows the BER performance against the SSPA parameter p at $E_b/N_0 = 8$ dB and $IBO = 0$ dB. The proposed compensator can compensate for the degradation due to nonlinear distortion and agrees well with theoretical result on the ML compensator.

In the previous analysis, the HPAs at the transmitter and receiver have the same input/output characteristic and the same back-off level. However, in practice, this assumption could be impossible, and a HPA characteristic and back-off level mis-matching will degrade the compensation performance. Figure 10 shows the BER performance against the input back-off error. The HPAs have the same input/output characteristic, but their back-off levels are different. The BER performance degrades with the increase of the input back-off error. However, the degradation due to the input back-off error is tolerable as compared with that due to nonlinear distortion. Figure 11 shows the BER performance against the error in parameter p. The proposed compensator is insensitive to the error in p. These results demonstrates that the proposed compensator for the SSPA is practical not only in a sense of the computational cost, but also in the accuracy of the compensator.

Figure 12 is the BER performance against E_b/N_0 at the input back-off level of 0 dB when applying the proposed compensation to 32-sub-carrier 16 QAM system. The BER performance of the proposed compen-

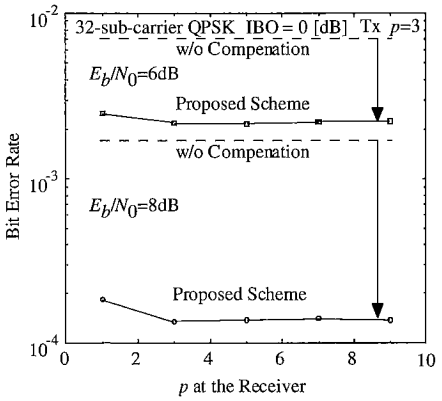

Fig. 11 Effect of the error in SSPA parameter p.

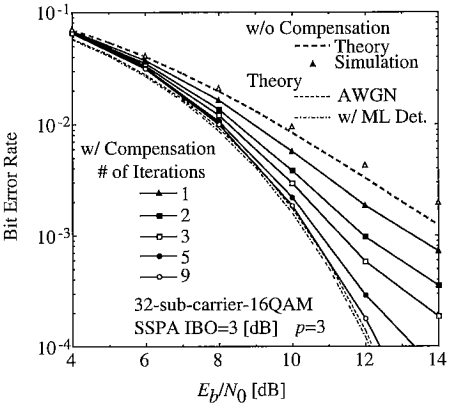

Fig. 12 Bit error rate performance of the proposed nonlinear distortion compensator for SSPA.

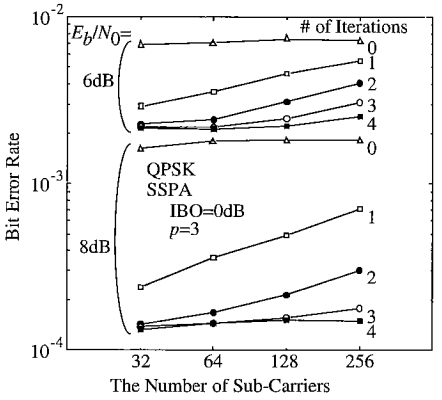

Fig. 13 Bit error rate performance against the number of sub-carriers.

sator agrees well with that of theoretical BER on the ML detection as well as the QPSK case. In the 16 QAM case, the proposed compensator can effectively compensate for the BER degradation due to the nonlinear distortion as well as in the case of QPSK.

Figure 13 is the BER performance of the QPSK system against the number of sub-carriers. The required number of iterations increases as the number of sub-carriers increases, since the expected number of error bits in the decoded sequence $\hat{B}^{(0)}$ is proportional to the number of sub-carriers. However, the proposed compensator is still effective when the number of sub-carriers is up to 256.

7. Conclusions

In this paper, we have proposed a new nonlinear distortion compensator based on maximum likelihood (ML) detection for orthogonal multi-carrier modulated signals. To reduce the computational cost required for the conventional ML detection, the proposed scheme employs a sub-optimum sequence estimation algorithm.

Theoretical analysis and computer simulation results show that the proposed scheme can compensate for the performance degradation due to nonlinear distortion. Furthermore, applying the proposed scheme iteratively, we can obtain a more improvement in the BER performance. The simulation results also show the proposed scheme is insensitive to the nonlinear HPA model error.

In this paper, we have only investigated the QPSK and 16 QAM systems, and only for a SSPA, namely, with no AM/PM conversion. In this sense, further investigations must be required using more sub-carriers and other type of non-linear amplifier such as a traveling wave tube amplifier (TWTA), namely, with AM/PM conversion.

Acknowledgments

The authors would like to thank Dr. Norihiko Morinaga, and Dr. Shinsuke Hara for fruitful discussions. The authors express thank Mr. Hiroshi Ishibashi for their assistance in computer simulation of our study.

References

[1] J.S. Chow, J. Tu, and J.M. Cioffi, "A discrete multitone transceiver system for HDSL applications," IEEE J. Select. Areas Commun., vol.9, no.6, pp.895–908, June 1991.
[2] B.L. Floch, R. Halbert-Lassalle, and D. Castelain, "Digital sound broadcasting to mobile receivers," IEEE Trans. Consum. Electron., vol.35, no.3, pp.493–503, Aug. 1989.
[3] H. Sari, G. Karam, and I. Jeanclaude, "Transmission techniques for digital terrestrial TV broadcasting," IEEE Commun. Mag., vol.33, no.2, pp.100–109, Feb. 1995.
[4] M. Okada, S. Hara, and N. Morinaga, "Bit error rate performances of orthogonal multicarrier modulation radio transmission system," IEICE Trans. Commun., vol.E76-B, no.2, pp.113–119, Feb. 1993.
[5] O. Simbo, "Transmission Analysis in Communication Systems," Computer Science Press, 1988.
[6] G. Santella and F. Mazzenga, "A model for performance evaluation in M-QAM-OFDM schemes in presence of nonlinear distortions," Proc. of IEEE VTC'95, pp.830–834, July 1995.
[7] M. Nagatsuka, A. Tsuzuku, and H. Fukuchi, "Effect of restrictions on instantaneous power of OFDM signal,"

IEICE Trans., vol.J78-B-II, no.6, pp.471–474, June 1995.
[8] S. Tomisato and H. Suzuki, "Multicarrier transmission system with low peak power for high bit-rate digital mobile radio communications," Proc. of the 1996 Commun. Society Conf of IEICE, vol.1, no.SB-3-4, pp.549–550, Sept. 1996.
[9] S. Komaki, K. Tsukamoto, and M. Okada, "Requirements for radio-wave photonic devices from the viewpoint of future mobile radio systems," IEEE Trans. Microwave Theory & Tech., vol.43, no.9, pp.2222–2228, Sept. 1995.
[10] L.D. Quach and S.P. Stapleton, "A postdistortion receiver for mobile communications," IEEE Trans. Veh. Technol., vol.42, no.4, pp.604–616, Nov. 1994.
[11] G. Satoh, "Nonlinear compensation techniques for analog optical transmission systems," IEICE Tech. Report, OMI96-7, July 1996.

Minoru Okada was born in Tokushima, Japan, on March 4, 1968. He received the B.E. degree in communications engineering from University of Electro-Communications, Tokyo, Japan, in 1990, and the M.E. degree in communications engineering, from Osaka University, Osaka, Japan, in 1992. He is currently an assistant professor in the Department of Communications Engineering at Osaka University. His current interest is in mobile radio communications systems. He is a member of IEEE.

Hideki Nishijima received the B.E. degree in electrical engineering, and the M.E. degree in communications engineering from Osaka University in 1995 and 1997, respectively. In 1997, he joined the NTT Kansai Mobile Communications Network, Inc. His research interest includes mobile communications.

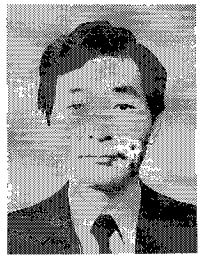

Shozo Komaki was born in Osaka, Japan, in 1947. He received B.E., M.E. and Ph.D. degrees in Electrical Communication Engineering from Osaka University, in 1970, 1972 and 1983 respectively. In 1972, he joined the NTT Radio Communication Labs., where he was engaged in repeater development for a 20-GHz digital radio system, 16-QAM and 256-QAM systems. From 1990, he moved to Osaka University, Faculty of Engineering, and engaging in the research on radio and optical communication systems. He is currently a Professor of Osaka University. Dr. Komaki is a senior member of IEEE, and a member of the Institute of Television Engineers of Japan (ITE). He was awarded the Paper Award and the Achievement Award of IEICE, Japan in 1977 and 1994 respectively.